Developmental Cognitive Neuroscience 10 (2014) 148–159

Contents lists available at ScienceDirect

Developmental Cognitive Neuroscience

journal homepage: http://www.elsevier.com/locate/dcn

Development of the Default Mode and Central Executive Networks across early adolescence: A longitudinal study

Lauren E. Sherman[a,b,*], Jeffrey D. Rudie[b], Jennifer H. Pfeifer[c], Carrie L. Masten[b], Kristin McNealy[b], Mirella Dapretto[b,d]

[a] Department of Psychology, University of California, Los Angeles, Los Angeles, CA, USA
[b] Ahmanson-Lovelace Brain Mapping Center, University of California, Los Angeles, Los Angeles, CA, USA
[c] Department of Psychology, University of Oregon, Eugene, OR, USA
[d] Department of Psychiatry and Biobehavioral Sciences, University of California, Los Angeles, Los Angeles, CA, USA

ARTICLE INFO

Article history:
Received 6 June 2014
Received in revised form 31 July 2014
Accepted 6 August 2014
Available online 20 August 2014

Keywords:
Adolescent brain development
Functional connectivity
Default Mode Network
Central Executive Network
Intelligence
Early adolescence

ABSTRACT

The mature brain is organized into distinct neural networks defined by regions demonstrating correlated activity during task performance as well as rest. While research has begun to examine differences in these networks between children and adults, little is known about developmental changes during early adolescence. Using functional magnetic resonance imaging (fMRI), we examined the Default Mode Network (DMN) and the Central Executive Network (CEN) at ages 10 and 13 in a longitudinal sample of 45 participants. In the DMN, participants showed increasing integration (i.e., stronger within-network correlations) between the posterior cingulate cortex (PCC) and the medial prefrontal cortex. During this time frame participants also showed increased segregation (i.e., weaker between-network correlations) between the PCC and the CEN. Similarly, from age 10 to 13, participants showed increased connectivity between the dorsolateral prefrontal cortex and other CEN nodes, as well as increasing DMN segregation. IQ was significantly positively related to CEN integration at age 10, and between-network segregation at both ages. These findings highlight early adolescence as a period of significant maturation for the brain's functional architecture and demonstrate the utility of longitudinal designs to investigate neural network development.

1. Introduction

Early adolescence is a period of substantial neural development, triggered in part by biological changes related to the onset of puberty as well as significant changes in youths' social sphere. Work in animals and neuroimaging studies in humans suggest that pubertal development corresponds with significant changes in the brains' structural and functional organization (e.g., Blakemore et al., 2010; Sato et al., 2008). This neural maturation is accompanied by developments in the social and cognitive domains. Adolescents experience a "social reorientation" (Nelson et al., 2005) whereby they become increasingly sensitive to social cues and peer relationships. Indeed, the emphasis on social learning and preparation for adult roles during adolescence occurs in cultures around the world (Schlegel and Barry, 1991; Schlegel, 1995). Youth also make important strides in executive functioning, including inhibitory control, planning for the future, metacognition, and hypothesizing about others' mental states (e.g., Dumontheil et al., 2010; Weil et al., 2013; Williams et al., 1999).

* Corresponding author at: 1285 Franz Hall, Box 951563, Los Angeles, CA 90095-1563, United States. Tel.: +1 215 317 4447.
E-mail address: lsherman@ucla.edu (L.E. Sherman).

http://dx.doi.org/10.1016/j.dcn.2014.08.002

Between childhood and adulthood, significant changes also occur in the functional architecture of the brain. The adult human brain is organized into functional networks, consisting of sets of distinct neural regions that demonstrate correlated blood oxygen level-dependent (BOLD) signal fluctuations both during specific tasks and while at rest (e.g., Fox and Raichle, 2007). Immature versions of these networks—i.e., significant but weaker connectivity between some or all "hub" regions of each network—have been documented in childhood and even, to some extent, in infancy (for a review, see Dennis and Thompson, 2013). Nonetheless, these immature networks tend to have weaker internal connectivity and are less functionally segregated (i.e., demonstrate stronger between-network correlation) than those in adulthood, with adolescence representing a period of intermediate connectivity (Jolles et al., 2011; Kelly et al., 2009; Fair et al., 2007a, 2009; Hwang et al., 2013). Despite our increasing understanding of the dramatic neural maturation that occurs during the second decade of life, relatively less is known about the development of functional networks *during* adolescence, particularly during the years when the most dramatic pubertal changes typically occur. Furthermore, the majority of research examining the maturation of functional networks has relied upon cross-sectional, rather than longitudinal data, with only a few exceptions in infant populations (e.g., Gao et al., 2014; Smyzer et al., 2010). The present study examines the development of two functional networks in early adolescence using a longitudinal sample of participants who were studied at ages 10 and 13. Specifically we examined the Default Mode Network (DMN) and the Central Executive Network (CEN), which have been implicated in social cognition and executive control, respectively.

Raichle and colleagues (2001) first observed that a network of neural regions, including the posterior cingulate cortex (PCC), the medial prefrontal cortex (mPFC), and the lateral parietal cortex showed increased activity during "baseline," or when an individual is at rest. This same network of regions has been shown to be deactivated during a variety of neuroimaging tasks requiring cognitive processing; indeed, it has also been labeled the "task-negative" network (Fox et al., 2005b; Greicius et al., 2003; Binder et al., 1999; Shulman et al., 1997). The past decade has seen a surge of scientific interest in the DMN, both in typical and clinical populations (for a review, see Broyd et al., 2009). In task-based fMRI designs, regions of the DMN are frequently activated during social cognition, including processing emotional stimuli, introspection, and thinking about others' mental states (e.g., Blakemore, 2008; Gusnard et al., 2001; Maddock, 1999). Given its involvement in social cognition, this network of regions is sometimes referred to as the "mentalizing network" in the social affective neuroscience literature (e.g., Atique et al., 2011).

The CEN, in contrast, is one of the two networks that frequently *activates* during typical fMRI tasks involving executive functions. Seeley and colleagues (2007) distinguished between the salience network, with main hubs in the dorsal anterior cingulate and orbitofrontal insular cortices, and the CEN, anchored in the dorsolateral prefrontal cortex (dlPFC) and posterior parietal cortex (pPC), particularly the intraparietal sulcus (IPS). They reported that activity in the CEN, but not the salience network, correlated with performance on executive control tasks. Emerging evidence suggests the strength of within-network connectivity in the CEN, (also called the frontoparietal control system/network; Vincent et al., 2008) is associated with higher IQ in children, adolescents, and adults (e.g., Langeslag et al., 2013; Li and Tian, 2014; Song et al., 2008). CEN activity has been shown to be anticorrelated with activity in the DMN in healthy adults (Fox et al., 2005b; Menon and Uddin, 2010; Sridharan et al., 2008), and it has been proposed that it may even directly inhibit DMN activity under certain circumstances (Chen et al., 2013). Data from cross-sectional research suggests that increasing integration within each functional network and segregation between these and other networks occurs throughout childhood and adolescence (Fair et al., 2007a).

The present study aimed to investigate the integration and segregation of the CEN and DMN during a relatively narrow period of development—ages 10 to 13—wherein significant structural and functional brain maturation, as well as socioemotional and cognitive development, occur. The data were collected as part of a longitudinal study which did not involve a traditional resting-state scan. Instead, we used functional data from a passive listening task of meaningless speech (McNealy et al., 2006, 2010, 2011) and performed the analyses on a residual timeseries after the task-specific effects were statistically controlled for. While our fMRI scan does differ somewhat from a traditional "resting state" scan, it is worth noting that participants were not engaging in active semantic processing, as the auditory stimulus was composed of unbroken nonsense syllables. Previous research has found that the brain's functional networks are detectable during task-based studies as well as at rest (Fair et al., 2007b; Harris et al., 2014; Smith et al., 2009). Indeed, work by Fox et al. (2005a) suggests that spontaneous fluctuations of functional networks account for a significant portion of the BOLD signal response during task-based fMRI paradigms. Our present findings demonstrate that the hubs of the DMN and CEN do indeed demonstrate significant and strong functional connectivity during a passive listening task, after controlling for the effects of that task (note that while the present study does not examine functional networks *as they relate* to language tasks, a growing body of literature considers this question; see, for example, Regev et al., 2013; Honey et al., 2012). In using a longitudinal dataset, we were afforded the ability to detect changes in functional connectivity with more sensitivity, and to conclude with greater confidence that our findings indeed reflect changes over time rather than differences between two samples. To the best of our knowledge, the present study is the first to use longitudinal data to examine the development of the brain's functional architecture during adolescence.

2. Methods

2.1. Participants

A sample of 45 typically developing children (24 females) participated in a longitudinal study on brain and

behavioral development during the adolescent years. All participants provided behavioral and neuroimaging data at two time points. At the first time point, participants ranged in age from 9.49 to 10.57 years (average age = 10.08 ± 0.31), and at the second time point ranged in age from 12.38 to 13.90 years (average age = 13.02 ± 0.32). Participants were ethnically and socioeconomically diverse: 53.3% of participants were White, 22.2% Hispanic, 6.7% Multiethnic/Multiracial, 6.7% Black, 4.4% Asian, 4.4% Native American/American Indian, and 2.2% Pacific Islander. Household income of the sample at age 10 (first time point) ranged from <$15,000 to >$400,000, with the median household income bracket $80,000–$100,000. Full-scale IQ, as assessed by the Wechsler Intelligence Scale for Children (WISC-III; Wechsler, 1991) ranged from 86 to 148 (Average IQ = 118.5). From age 10 to 13 (first to second time point), the 45 participants did not differ in their level of mean absolute motion ($p = .205$), maximum absolute motion ($p = .408$), mean relative motion ($p = .458$), and maximum relative motion ($p = .627$). Participants' average score on the Pubertal Development Scale (PDS; Petersen et al., 1988) was 1.79 at age 10 and 2.65 at age 13 (out of a possible four points). The PDS measures puberty through a series of self-report questions assessing physical changes. For example, items on the PDS assess changes in body and facial hair growth and voice changes for males, and increases in breast size and onset of menarche for females. Responses of "1" correspond to the prepubertal stage and "4" correspond to the post-pubertal stage. At age 10, none of our female participants reported having experienced menarche; at age 13, 64% of our female participants reported that they had experienced menarche. Indeed, at age 13, none of our participants reported being completely post-pubertal (i.e., with a score of 4 points), but all reported experiencing at least some changes as a result of puberty. Participants had no history of significant medical, psychiatric, or neurological disorders. Participants and their parents completed written consent and assent in accordance with the university's Institutional Review Board and were compensated for their participation.

2.2. fMRI paradigm and data acquisition

Data used in the present study were acquired during an fMRI scan lasting 8 min and 48 s. Participants passively listened to a stream of nonsense speech (concatenated syllables). Participants were not explicitly instructed to perform any task other than listening to the syllables. The nonsense speech was presented in three counterbalanced blocks (McNealy et al., 2006, 2010, 2011).

Functional and structural images were acquired using a Siemens Allegra 3 Tesla head-only MRI scanner. A two-dimensional spin-echo scout [repetition time (TR), 4000 ms; echo time (TE), 40 ms; matrix size, 256 × 256; 4 mm thick; 1 mm gap] was acquired in the sagittal plane to allow prescription of the slices to be obtained in the remaining scans. For each participant, a high-resolution structural T2-weighted echo-planar imaging (EPI) volume [TR, 5000 ms; TE, 33 ms; matrix size, 128 × 128; field of view (FOV), 20 cm; 36 slices; 1.56 mm in-plane resolution; 3 mm thick] was acquired coplanar with the functional scans to allow for spatial registration of each participant's data into a standard coordinate system. For the speech stream exposure task, one functional scan was acquired covering the whole cerebral volume (174 images; EPI gradient echo sequence; TR, 3000 ms; TE, 25 ms; flip angle, 90°; matrix size, 64 × 64; FOV, 20 cm; 36 slices; 3.125 mm in-plane resolution; 3 mm thick; 1 mm gap).

2.3. fMRI data preprocessing

fMRI data were preprocessed and analyzed using FSL version 4.1.4 (FMRIB's Software Library, http://www.fmrib.ox.ac.uk/fsl; Smith et al., 2004) and AFNI (Analysis of Functional NeuroImages; Cox, 1996). Structural images were skull-stripped using AFNI's 3dskullstrip and functional images were skull stripped using AFNI's 3dautomask. Functional volumes were motion corrected to the average functional volume using MCFLIRT (Jenkinson et al., 2002), which utilizes a normalized correlation ratio cost function and sinc interpolation. Translations and rotations in the x, y, and z dimensions were calculated from volume to volume and then collapsed into mean absolute (compared with the average functional volume) and relative (compared with the previous volume) displacements.

2.3.1. fMRI analysis with motion scrubbing

An ongoing concern in functional connectivity studies, particularly in developmental populations, is the potential bias caused by head motion in the scanner. Several research groups (e.g., Power et al., 2012; Satterthwaite et al., 2012; van Dijk et al., 2012) have demonstrated that even minimal differences in motion between two samples can introduce artifacts into the data. Several procedures have recently been proposed to addressed these motion confounds. Power and colleagues (2012) recommend "scrubbing," or completely removing volumes of data during which excessive motion or motion-related signal changes are observed, as well as volumes preceding and following these outlier volumes. Others (Hallquist et al., 2013; Satterthwaite et al., 2013) suggest applying a bandpass filter, employed to remove artifacts created by high and low-frequency noise, either after regressing nuisance variables or simultaneously with this step. Importantly, work by Satterthwaite and colleagues (2013) suggests that, after taking into account the biases introduced by motion artifacts, functional connectivity continues to be a valid and valuable approach to characterizing neurodevelopment across the lifespan. Given the ongoing debate about motion artifacts, particularly in developmental populations, we have elected to perform analyses in two ways to confirm that our main findings survive rather different analytic approaches: (1) using our original pipeline, but applying motion scrubbing and (2) reversing the bandpass filter and nuisance regression steps, without motion scrubbing. The Methods and Results for the latter analyses are presented in our Supplementary materials. Here, we present our original pipeline which included motion scrubbing.

Time-series statistical analysis was carried out according to the general linear model using FEAT (FMRI Expert

Analysis Tool), Version 5.98. Following preprocessing, a temporal band pass filter (0.01 Hz < t < 0.1) was applied to each subject's data. Images were then spatially smoothed using a Gaussian kernel of FWHM 5 mm, and the language task was entered as a regressor into the model. FAST (FSL's Automatic Segmentation Tool) was used to generate individual subject masks for cerebrospinal fluid (CSF), white matter (WM) and global signal from their structural images. We performed nuisance regression using these WM, CSF, and global signal masks. Based on Power and colleagues' (2012) recommendation, we did not include motion parameters as nuisance regressors in the model.

Next, utilizing the steps recommended by Power and colleagues (2012), we calculated each participant's framewise displacement (FD), a scalar measurement of motion using the six rigid body motion parameters, and a global measure of volume-to-volume BOLD image intensity change (DVARS; D referring to temporal derivative of timecourses, VARS referring to the root mean square of variance over voxels). Volumes in which FD exceeded 0.5 and DVARS exceeded 0.5% change in the BOLD signal (Power et al., 2012) were "scrubbed," or removed entirely from the data. Furthermore, to account for the temporal smoothing of BOLD data in functional connectivity processing, the volume preceding and two volumes immediately following the "scrubbed" volume were also removed. On average, a total of 11.53 volumes were removed from age 10 data and 11.36 volumes were removed from age 13 data. A paired t-test revealed that the number of volumes scrubbed at ages 10 and 13 were not significantly different, $t(44) = 0.07$, $p = .947$.

These "scrubbed" residuals were aligned to subjects' high-resolution coplanar images via an affine transformation with 6 degrees of freedom. We then used FMRIB's linear image registration tool (FLIRT) to align the residuals to the standard Montreal Neurological Institute (MNI) average brain using an affine transformation with 12 degrees of freedom.

In order to examine whole-brain connectivity in the DMN and CEN, we selected two seed regions based on findings from the existing literature and performed seed-based connectivity analyses. To examine the DMN, we selected a spherical seed in the posterior cingulate cortex (PCC) based on Shulman and colleagues' 1997 meta-analysis (MNI coordinates −5, −53, 41; see also von dem Hagen et al., 2013). Previous research (Margulies et al., 2009) has detected heterogeneity in the functional connectivity of the precuneus and PCC using multiple 3-mm spherical seeds. Given this heterogeneity, as well as the heterogeneity of individual participants' anatomy, we elected to use a relatively large 10-mm seed in order to elicit a broader connectivity map, though more targeted seeds may be appropriate in the future as our understanding of the development of the DMN progresses. To examine the CEN, we selected a 10 mm-diameter spherical seed in the dorsolateral prefrontal cortex (dlPFC), using coordinates identified by Seeley and colleagues as uniquely differentiating the CEN from the salience network (MNI coordinates 44, 36, 20). We extracted ROI time-series from each subject's processed residuals in standard space and correlated them with every voxel in the brain to generate connectivity maps for each subject and ROI. Individual correlation maps were then converted into z-statistic maps using Fischer's r to z transformation. At the group level, we modeled a paired-sample mixed-effects design ($Z > 2.3$, corrected for multiple comparisons at the cluster level $p < .05$), and compared connectivity in each of the networks at ages 10 and 13. To examine the possible role of IQ in predicting individual differences in the CEN, we performed two additional mixed-effect analyses ($Z > 2.3$, corrected for multiple comparisons at the cluster level $p < .05$) relating participants' full-scale IQ, as measured by the WISC at age 10 to dlPFC connectivity across the whole brain (at both age 10 and 13). Participants completed the Wechsler Abbreviated Scale of Intelligence (WASI; Wechsler, 1999), but not the full WISC, at age 13. While some research has documented changes in IQ scores during late childhood/early adolescence (Canivez and Watkins, 1998; Watkins and Smith, 2013), our participants' WISC scores at age 10 and their WASI scores at age 13 were highly correlated ($r = .75$, $p < .00001$). We elected to use scores from the more comprehensive WISC in our analyses.

3. Results and discussion

3.1. Default mode and central executive networks at ages 10 and 13

Fig. 1 depicts the DMN (panels A and B) and CEN (panels E and F) as identified in our samples at ages 10 and 13. At both time points, participants' functional networks resembled those found in mature adults in previous work (e.g., Raichle et al., 2001; Seeley et al., 2007): the "hub" regions described in previous work were significantly correlated with our seed regions as described below.

Activity in the PCC seed was significantly correlated with other "hub" regions of the DMN, including the mPFC and the lateral parietal lobules (Raichle et al., 2001). Additionally, Table 1 describes a number of other regions showing correlated activity with the DMN, including the caudate, thalamus, bilateral temporal cortex, and cingulate, among others. Notably, the left hippocampus and left frontal orbital cortex showed significant connectivity with the PCC at age 13 but not age 10.

Activity in the dlPFC seed was significantly correlated with "hub" regions of the CEN, including those located in the dmPFC and IPS (Seeley et al., 2007). Other regions demonstrating correlated activity with the seed, including the bilateral superior and inferior temporal gyri and the bilateral insula, are detailed in Table 2. Two regions—the left cerebellum and the left inferior temporal gyrus—were significantly correlated with the dlPFC at age 13 but not age 10.

Other researchers have not always found that the functional networks of late childhood or early adolescence resemble those in adulthood so closely. For example, Fair and colleagues (2008) reported that among slightly younger children (ages 7–9), the medial prefrontal cortex was only minimally connected to the PPC and the lateral parietal cortices, whereas we found robust connections between the mPFC and PPC. It is possible that significant maturation between ages 7–9 and age 10 account for

Table 1
Peak coordinates of Default Mode Network connectivity maps for posterior cingulate seed.

	Age 10					Age 13					10 > 13					13 > 10				
	MNI peak (mm)			Max *Z*	Sig # voxels	MNI peak (mm)			Max *Z*	Sig # voxels	MNI peak (mm)			Max *Z*	Sig # voxels	MNI peak (mm)			Max *Z*	Sig # voxels
	x	*y*	*z*			*x*	*y*	*z*			*x*	*y*	*z*			*x*	*y*	*z*		
Medial prefrontal cortex	4	48	22	6.94	16,307	2	50	20	8.17	18,105						18	34	22	4.30	1558
Ventromedial prefrontal cortex	4	50	−12	7.00		−2	50	−8	7.92											
Dorsomedial prefrontal cortex	22	32	48	6.70		22	32	48	6.69							10	54	42	4.18	
Left middle frontal gyrus	−30	22	44	6.98		−26	22	46	7.66							−14	42	36	2.90	
Right middle frontal gyrus	22	30	42	8.17		20	32	44	7.44		30	8	44	3.12	13					
Right frontal orbital cortex	36	18	−20	3.84	50	32	16	−18	4.96	160										
Left frontal orbital cortex						−32	12	−14	4.19	245										
Right caudate	12	24	−4	2.93	11	6	8	0	3.17	12										
Left caudate	−6	12	−2	3.73	32	−6	8	−2	3.81	100										
Thalamus	−10	−32	10	4.45	90	−10	−34	10	5.34	379										
Left Hippocampus/parahippocampal gyrus						−24	−36	−14	6.02	653						−20	−24	−18	4.59	251
Anterior cingulate	10	32	−4	5.96	1036	2	46	4	7.21	1500						16	34	20	3.98	193
Posterior cingulate/precuneus	0	−56	38	12.75	11,338	−8	−56	40	11.66	11,632	20	−48	34	3.19	40	−4	−60	8	3.98	630
Right temporal cortex	54	0	−26	6.71	2971	56	0	−22	7.57	2647										
Left temporal cortex	−60	−10	−18	6.80	2865	−58	−16	−14	7.14	3225						−58	−6	−16	3.85	322
Right lateral parietal cortex	46	−66	40	8.11	4084	52	−58	28	8.50	3087	34	−56	30	3.28	76					
Left lateral parietal cortex	−48	−58	28	8.99	4930	−50	−68	32	8.81	4542										
Right cerebellum	6	−52	−46	5.38	807	32	−78	−34	6.24	1431										
Left cerebellum	−6	−52	−46	6.07	479	−6	−50	−42	5.90	1102										

Coordinates are in Montreal Neurological Institute space. Results for 10 > 13 and 13 > 10 depict activity that overlaps with the Default Mode Network in the sample at Time 2 (age 13). For all maps, $Z > 2.3$, cluster corrected for multiple comparisons at $p < .05$.

Table 2
Peak coordinates of Central Executive Network connectivity maps for dorsolateral prefrontal cortex seed.

	Age 10				Age 13					10 > 13					13 > 10				
	MNI peak (mm)			Max *Z*	Sig # voxels	MNI peak (mm)			Max *Z*	Sig # voxels	MNI peak (mm)			Max *Z*	Sig # voxels	MNI peak (mm)			Max *Z*	Sig # voxels
	x	*y*	*z*			*x*	*y*	*z*			*x*	*y*	*z*			*x*	*y*	*z*		
Right dorsolateral prefrontal cortex	46	40	18	11.03	14,444	46	36	20	12.39	13,159						48	36	24	4.61	654
Right lateral prefrontal cortex	38	48	8	8.43		46	48	4	8.66							46	52	6	4.23	
Left dorsolateral prefrontal cortex	−46	34	26	7.33	5889	−40	32	18	7.06	4749										
Left lateral prefrontal cortex	−38	38	6	6.38		−40	38	6	6.82											
Dorsomedial prefrontal cortex	4	20	44	5.76	1439	6	20	42	8.10	1757						4	20	44	4.07	389
Right insular cortex	30	20	6	6.87	959	32	22	0	8.00	1217										
Left insular cortex	−28	16	8	5.10	431	−30	18	6	6.40	624										
Left putamen	−22	−4	4	5.32	555	−28	16	6	5.68	556										
Right putamen	30	18	4	7.04	1048	32	16	4	7.85	1223										
Cingulate	4	−8	28	3.66	314	0	2	28	5.39	729										
Right caudate	14	10	8	5.03	142	14	−4	18	5.80	120										
Left caudate	−12	10	6	4.15	43	−14	−6	18	4.75	42										
Thalamus	10	−16	10	4.68	272	10	−14	10	5.55	466										
Right planum temporale/superior temporal gyrus	52	14	−6	4.10	243	52	10	−6	5.74	1118										
Left planum temporale/superior temporal gyrus	−46	−20	10	3.32	53	−54	−38	22	4.28	619										
Right inferior temporal gyrus	54	−50	−4	5.99	992	56	−38	−14	5.73	1246										
Left inferior temporal gyrus						−50	−48	−12	4.00	246										
Left posterior parietal cortex	−46	−42	46	5.57	3237	−46	−40	42	6.45	2251										
Left lateral occipital cortex	−32	−64	58	4.80		−28	−66	40	4.42											
Right posterior parietal cortex	56	−38	52	8.09	7038	50	−42	54	8.74	6475						42	−60	58	4.14	707
Right lateral occipital cortex	32	−64	44	5.69		32	−62	40	7.08							46	−60	54	2.51	
Left cerebellum						−10	−80	−32	5.79	1647						−30	−74	−50	4.67	813

Coordinates are in Montreal Neurological Institute space. Results for 10 > 13 and 13 > 10 depict activity that overlaps with the Central Executive Network in the sample at Time 2 (age 13). For all maps, $Z > 2.3$, cluster corrected for multiple comparisons at $p < .05$.

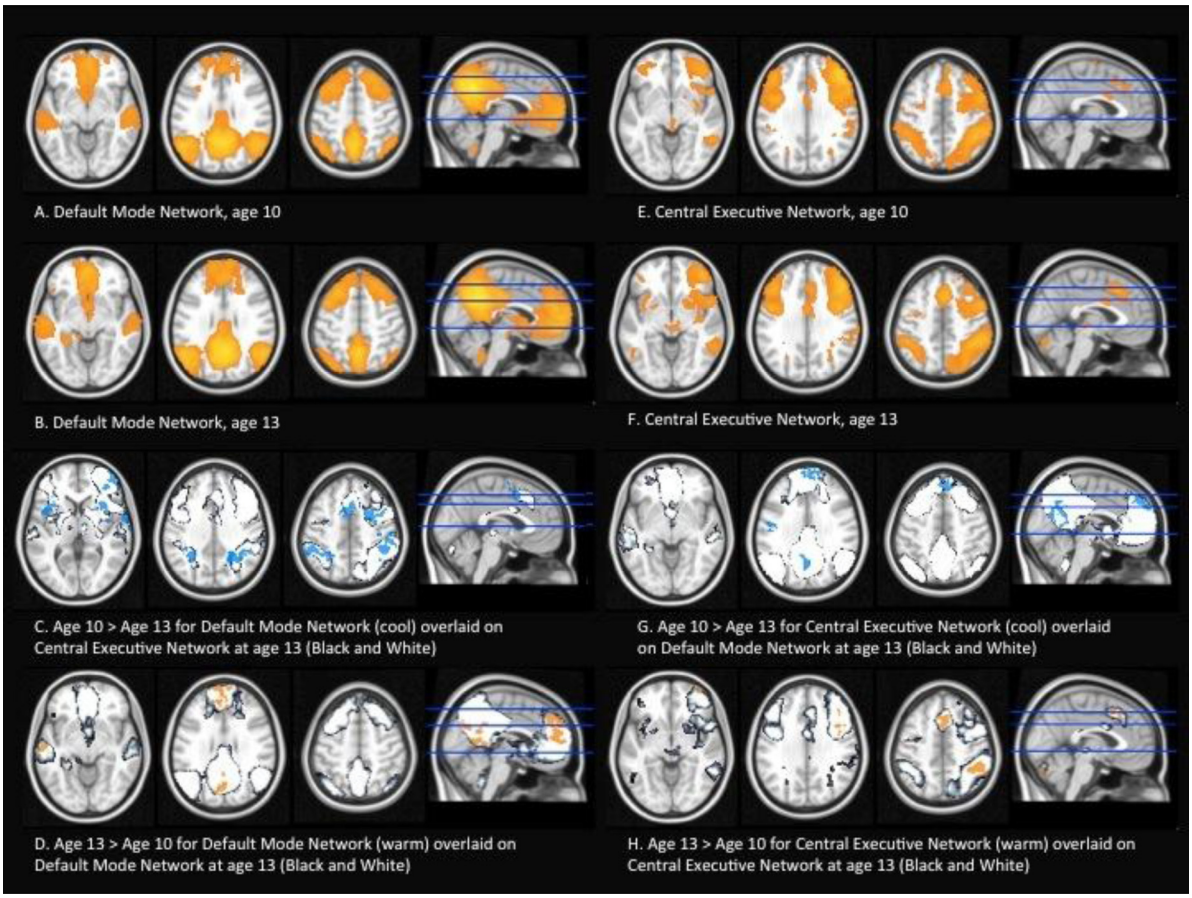

Fig. 1. Panels A and B depict connectivity maps for the Default Mode Network (DMN) seed at ages 10 and 13, respectively. Panel C depicts DMN-seed connectivity that was greater at age 10 relative to age 13, overlaid on the more mature Central Executive Network (CEN) connectivity map to illustrate the considerable overlap between them. Panel D depicts DMN-seed connectivity that was greater at age 13 relative to age 10, overlaid on the more mature DMN connectivity map. Panels E and F depict connectivity maps for the CEN seed at ages 10 and 13 respectively. Panel G depicts CEN-seed connectivity greater at age 10 relative to age 13, overlaid on the more mature DMN connectivity map to highlight network overlap. Panel H depicts CEN-seed connectivity greater at age 13 than age 10, overlaid upon the more mature CEN connectivity map.

differences in our findings. Additionally, differences in seed regions (Fair and colleagues used a seed in the mPFC), preprocessing, and motion correction may also account for the discordant findings, as could the fact that Fair and colleagues utilized a traditional resting state scan whereas our participants passively listened to a meaningless speech stream. Nonetheless, our findings suggest that by age 10, the basic functional architecture of the DMN is in place. Less is known about the developmental timecourse of the CEN, but our findings suggest that this, network, too is largely functionally connected by age 10.

3.2. Increasing connectivity within networks

While both networks do appear to be largely functionally connected by age 10, we observed significant changes from age 10 to 13 suggesting that connectivity within the DMN and CEN continues to strengthen internally through early adolescence. Fig. 1 (panel D) depicts regions that increased in PCC connectivity from age 10 to 13. We observed an increase in connectivity between the PPC and the mPFC, two important hubs of the DMN and, notably, a particularly long-range connection. Table 1 details regions of the DMN, as defined in our sample at age 13, that either increased or decreased in connectivity from the first to the second time point. Seven regions increased in connectivity with our seed over time, including the left hippocampus, the left middle frontal gyrus, the anterior cingulate, and left temporal cortex. In comparison, three regions of considerably smaller size showed greater seed-region connectivity age 10: the right middle frontal gyrus and the right lateral parietal cortex and a portion of the precuneus located ventral to the seed. Increased DMN integration has been observed in previous cross-sectional work comparing children, adolescents, and adults (Fair et al., 2007a, 2008; Supekar et al., 2010; Uddin et al., 2011). Our longitudinal results, over a narrower age range, suggest that early adolescence may be a particularly important period during which this integration occurs. In particular, our finding suggesting significant increases in PCC-mPFC connectivity is consistent with the findings of Supekar and colleagues (2010), suggesting that while bilateral temporal regions of

the DMN already show strong functional connectivity to one another and to the PCC by late childhood, the mPFC-PCC connection continues to develop significantly from late childhood to young adulthood (see also Fair et al., 2007a). Indeed, Supekar and colleagues also documented significant differences in the dorsal cingulum "cingulate gyrus" tract, which connects the PCC and mPFC, suggesting a structural explanation for the protracted developmental trajectory of these particular neural regions. Furthermore, in a sample of 9–13 year olds, Gordon and colleagues (2011) found that DMN functional connectivity related positively to white matter integrity in this network.

Fig. 1 (panel H) depicts regions showing increased connectivity from age 10 to 13 between our CEN seed region, the dlPFC, and several other regions implicated in this network, including the right IPS and dmPFC, as well as the cerebellum. In contrast, no regions of the CEN (as defined in our sample at age 13) showed significant decreased connectivity with the dlPFC seed over time. As with the DMN, these results highlight the extent to which network maturation occurs in early adolescence. These findings are also consistent with previous work examining a wider age range: Fair and colleagues (2007a) found that the connection between the dlPFC and the IPS increased between late childhood (age range 7–9 years) and adolescence (age range 10–15 years), and that the connection between the dlPFC and cerebellum increased significantly from late childhood to adulthood.

3.3. Increasing segregation between networks

The strengthening of within-network connections is only one aspect of functional network maturation; the two networks also become increasingly segregated throughout early adolescence. Fig. 1 (panel C) depicts regions for which connectivity was greater at age 10 than age 13. In many cases, this change represented an *increase* in negative connectivity over time (i.e., greater anticorrelation). Regions with significant negative DMN-connectivity that became increasingly anticorrelated with the DMN from age 10 to 13 included hubs of the CEN, such as the pPC and the dmPFC. Fig. 1 (panel C) shows that the regions of increasing negative DMN-seed connectivity overlap considerably with CEN regions as identified in our sample at age 13. Similarly, regions of increasing anticorrelation with the CEN seed were amongst those showing greater positive connectivity over time within the DMN (Fig. 1, panel G). In particular, both the mPFC and the PCC demonstrated increased negative connectivity with the dlPFC seed.

In adult populations, the DMN and CEN have been described as "intrinsically anticorrelated" (Fox et al., 2005b). Some (e.g., Anderson et al., 2011; Murphy et al., 2009) have suggested that this anticorrelation arises as a direct result of global signal regression and is, therefore, not intrinsic at all but rather an artifact of this particular analytic technique. However, anticorrelated networks have been documented using functional connectivity techniques that do not incorporate global signal regression (Beckmann et al., 2005; Chang and Glover, 2009). Furthermore, it is likely that global signal fluctuations obscure both negative and positive correlations, necessitating their regression in functional connectivity analyses (Fox et al., 2009). A recent analysis in macaques found that inclusion of the global signal increased the relationship between underlying structural and functional connectivity, suggesting the global signal may serve to refine functional data (Miranda-Dominguez et al., 2014). Thus, we elected to implement global signal regression in the present analyses. With this debate in mind, however, the exact magnitude of the negative relationship between the CEN and DMN should be interpreted cautiously.

Our findings are consistent with others suggesting that greater segregation—be it weaker positive correlation or stronger anticorrelation—between individual networks occurs with age (Dosenbach et al., 2010; Fair et al., 2007a, 2009; Thomason et al., 2008). In particular, Stevens et al. (2009) found increasing segregation in the multiple default-mode and prefrontal-partietal attention circuits they identified using ICA analysis in a cross-sectional sample of participants aged 12–30. Using a longitudinal sample, we demonstrate that some of these age-related differences can be specifically attributed to maturation that occurs within the narrow window of early adolescence.

Unlike many other studies exploring developmental changes in network integration and segregation across the entire brain (e.g., Dosenbach et al., 2010; Fair et al., 2009; Stevens et al., 2009), we elected to narrow our focus to two particular networks. Sonuga-Barke and Castellanos (2007) proposed that the DMN and the "task positive" network, which encompasses the CEN among other regions, can be conceptualized as a single network consisting of anticorrelated parts. Considered within this framework, our findings suggest that early adolescence is a period during which the two individual components of this complex network mature, as well as a period in which these components become increasingly defined by their contrast to one another. Dosenbach and colleagues (2010) found that from age 7 to 30, increases in negative connectivity are significantly better predictors of age than increases in positive connectivity. Our findings suggest that during early adolescence, this segregation is a vital aspect of network maturity. Indeed, some areas that increased significantly in *negative* connectivity with our DMN seed (e.g., the dmPFC and pPC), were the same areas that increased significantly in positive connectivity with our CEN seed, and vice versa.

3.4. Functional connectivity in the CEN and intelligence quotient

At age 10, IQ was found to modulate connectivity between the dlPFC (our CEN hub) and another region of the CEN, the pPC, such that higher IQ was associated with stronger connectivity (MNI peak voxel coordinates $x = 64$, $y = -34$, $z = 46$, max $Z = 4.17$, 351 voxels; see Supplementary Fig. 2). Note that while IQ correlated with participants' mean absolute and relative head motion at age 10, IQ predicted positive dlPFC-pPC connectivity over and above the influence of both measures of motion ($p < .001$). At age 10, IQ was significantly negatively correlated with connectivity between the dlPFC and two regions: (1) a frontal region encompassing the subcallosal cortex and the

nucleus accumbens (MNI peak voxel coordinates, $x = -8$, $y = 8$, $z = -12$, max $Z = 4.57$, 306 voxels) which overlapped partially with the DMN as identified in our sample at both time points; (2) a region in the precuneus/PCC (MNI peak voxel coordinates $x = -12$, $y = -50$, $z = 18$, max $Z = 4.01$, 368 voxels) belonging to the DMN. The negative relationship observed between IQ and connectivity between these regions remained significant after controlling for absolute and relative mean head motion ($p < .001$). Supplementary Fig. 2 demonstrates the extent to which these regions overlap with the DMN.

At age 13, IQ was not positively correlated with dlPFC connectivity. However, IQ was negatively correlated with connectivity between the dlPFC and a region in the vmPFC that overlapped with the DMN (MNI peak voxel coordinates $x = 12$, $y = 32$, $z = -12$, $Z = 4.93$, 399 voxels; see Supplementary Fig. 2), and this effect was significant over and above the combined influence of relative and absolute mean head motion ($p < .001$).

Our findings are consistent with previous cross-sectional work examining the relationship between IQ and network connectivity in children and adolescents using an ICA approach. Langeslag and colleagues (2013) found a significant positive correlation between IQ and connectivity in the right PFC and pPC in a sample of 6–8 year olds. Li and Tian (2014) examined the relationship between the right and left frontoparietal control networks and IQ in childhood and adolescence: they also found that connectivity strength in regions of the right network were positively associated with IQ. Other research also suggests that the relation between IQ and connectivity in the CEN or frontoparietal networks persists into adulthood. Song and colleagues (2008) utilized a functional connectivity approach that most closely resembled ours: in an adult sample, they examined connectivity with bilateral dlPFC seeds. They too found a relation between IQ and positive connectivity in the right dlPFC and right pPC. They also reported significant negative correlations between IQ and connectivity between the dlPFC and non-CEN regions (e.g., the cuneus and lingual gyrus), though these regions were different than those we identified. Others have demonstrated that IQ relates to other measures of connectivity, including global efficiency and regional homogeneity (van den Heuvel et al., 2009; Santarnecchi et al., 2014; Wang et al., 2011).

Like the literature cited above, our findings support the hypothesis forwarded by Jung and Haier (2007) suggesting that individual differences in the structure and function of the frontoparietal regions implicated in the CEN are meaningfully related to variability in human intelligence. By using a seed-based whole-brain analysis, we were also able to examine which regions *outside* of the CEN showed dlPFC connectivity that was positively or negatively correlated with IQ. In support of the importance of network integration, there were no regions outside of the CEN that had dlPFC connectivity that was significantly positively related to IQ. In support of the importance of network segregation, dlPFC connectivity with regions *outside* of the CEN was negatively correlated with IQ. Of note, two of these regions—the PCC and the vmPFC—represent important hubs of the DMN. In other words, higher IQ was related to greater between-network segregation. Ultimately our findings suggest that elements of functional network integration and segregation witnessed across development also relate to individual differences in intellectual performance.

4. Conclusions, limitations, and future directions

We observed significant within-network maturation (i.e., stronger within-network connectivity) and between-network segregation (i.e., weaker correlation between regions belonging to different networks) in the brain's functional architecture from ages 10 to 13. This relatively brief age gap is nonetheless a particularly significant one for physical, neural, and social development. Our findings suggest that this developmental period may also be particularly important for functional maturation. Further, we observed a relationship between connectivity with our CEN seed and IQ. At age 10, within-network integration in the CEN (i.e., dlPFC-pPC connectivity) was significantly positively associated with IQ. Less segregation between the dlPFC seed and non-CEN regions—including the PCC, a hub of the DMN—was associated with lower IQ at both age 10 and age 13. Taken together, our longitudinal findings and the correlations with IQ suggest that a complete understanding of network maturity and efficiency must take into account not only individual networks but also the relationships between them.

Some limitations of the present study must be noted. While the field has converged on some general practices for analyzing functional connectivity data, debate as to the best practices is ongoing with new techniques and approaches continuing to emerge. In presenting findings resulting from two analytic approaches, we aimed to demonstrate that our main findings—that is, the increased integration and segregation of functional networks over a relatively short period of adolescence—are indeed robust to two such different approaches. Another limitation of note is our use of data collected during a passive-listening fMRI scan, rather than a traditional resting-state scan. Future research replicating the present findings with traditional resting-state data is needed to corroborate our conclusions and allow for easier comparison between these results and others employing traditional resting state. Nonetheless, in using the present dataset, we were afforded the opportunity to examine the maturation of functional networks longitudinally. To the best of our knowledge, no published research has investigated functional networks during this developmental epoch using a longitudinal design, despite the considerable increase in power provided by such an approach.

The majority of the extant literature on the development of the DMN and CEN has taken a broader approach, comparing functional networks between children and adolescents, or even children and adults. Our results suggest that it is indeed feasible to narrow the focus to briefer periods in adolescence, particularly those in which considerable structural maturation is known to occur. This research has implications for our understanding of the trajectory of altered connectivity in developmental disorders and delays. In a recent review of the development of

brain connectivity in autism, Uddin et al. (2010) suggest that the diverse and often conflicting findings regarding brain connectivity in autism may be somewhat ameliorated by a more fine-tuned understanding of how networks change *throughout* childhood and adolescence, particularly during puberty and particularly using longitudinal samples. In gaining greater understanding of typical development during this period, we pave the way for research targeting at-risk and atypical populations. Furthermore, we can begin to connect the maturation of functional networks with the substantial social and cognitive developments that occur during the second decade of life. Our findings demonstrate the importance of considering both connections within each network as well as the extent to which individual networks are segregated. Continued research characterizing the development of functional brain networks will allow us to better understand how such development relates to the vast array of other changes that occur throughout adolescence.

Conflict of interest

The authors declare no conflict of interest.

Acknowledgements

This work was supported in part by the Santa Fe Institute Consortium. Support was also provided by an FPR-UCLA Center for Culture, Brain, and Development Award (to L.S.). The authors are also grateful for the generous support from the Brain Mapping Medical Research Organization, Brain Mapping Support Foundation, Pierson–Lovelace Foundation, Ahmanson Foundation, Tamkin Foundation, Jennifer Jones–Simon Foundation, Capital Group Companies Charitable Foundation, Robson Family, William M. and Linda R. Dietel Philanthropic Fund at the Northern Piedmont Community Foundation, and Northstar Fund. This project was also partially supported by grants (RR12169, RR13642 and RR00865) from the National Center for Research Resources, a component of the National Institutes of Health.

Appendix A. Supplementary data

Supplementary material related to this article can be found, in the online version, at http://dx.doi.org/10.1016/j.dcn.2014.08.002.

References

Anderson, J.S., Druzgal, T.J., Lopez-Larson, M., Jeong, E.-K., Desai, K., Yurgelun-Todd, D., 2011. Network anticorrelations, global regression, and phase-shifted soft tissue correction. Hum. Brain Mapp. 32 (6), 919–934, http://dx.doi.org/10.1002/hbm.21079.

Atique, B., Erb, M., Gharabaghi, A., Grodd, W., Anders, S., 2011. Task-specific activity and connectivity within the mentalizing network during emotion and intention mentalizing. Neuroimage 55 (4), 1899–1911, http://dx.doi.org/10.1016/j.neuroimage.2010.12.036.

Beckmann, C.F., DeLuca, M., Devlin, J.T., Smith, S.M., 2005. Investigations into resting-state connectivity using independent component analysis. Philos. Trans. R. Soc. Lond. B: Biol. Sci. 360 (1457), 1001–1013, http://dx.doi.org/10.1098/rstb.2005.1634.

Binder, R., Frost, J.A., Hammeke, T.A., Bellgowan, P.S.F., Rao, S.M., Cox, R.W., 1999. Conceptual processing during the conscious resting state: a functional MRI study. J. Cogn. Neurosci. 11 (1), 80–93, http://dx.doi.org/10.1162/089892999563265.

Blakemore, S.-J., 2008. The social brain in adolescence. Nat. Rev. Neurosci. 9 (4), 267–277, http://dx.doi.org/10.1038/nrn2353.

Blakemore, S.J., Burnett, S., Dahl, R.E., 2010. The role of puberty in the developing adolescent brain. Hum. Brain Mapp. 31 (6), 926–933.

Broyd, S.J., Demanuele, C., Debener, S., Helps, S.K., James, C.J., Sonuga-Barke, E.J.S., 2009. Default-mode brain dysfunction in mental disorders: a systematic review. Neurosci. Biobehav. Rev. 33 (3), 279–296, http://dx.doi.org/10.1016/j.neubiorev.2008.09.002.

Canivez, G.L., Watkins, M.W., 1998. Long-term stability of the Wechsler intelligence scale for children—third edition. Psychol. Assess. 10 (3), 285–291, http://dx.doi.org/10.1037/1040-3590.10.3.285.

Chang, C., Glover, G.H., 2009. Effects of model-based physiological noise correction on default mode network anti-correlations and correlations. Neuroimage 47 (4), 1448–1459, http://dx.doi.org/10.1016/j.neuroimage.2009.05.012.

Chen, A.C., Oathes, D.J., Chang, C., Bradley, T., Zhou, Z.-W., Williams, L.M., Glover, G.H., Deisseroth, K., Etkin, A., 2013. Causal interactions between fronto-parietal central executive and default-mode networks in humans. Proc. Natl. Acad. Sci. U. S. A., 201311772, http://dx.doi.org/10.1073/pnas.1311772110.

Cox, R.W., 1996. AFNI: software for analysis and visualization of functional magnetic resonance neuroimages. Comput. Biomed. Res. 29 (3), 162–173.

Dennis, E.L., Thompson, P.M., 2013. Mapping connectivity in the developing brain. Int. J. Dev. Neurosci. 31 (7), 525–542, http://dx.doi.org/10.1016/j.ijdevneu.2013.05.007.

Dosenbach, N.U.F., Nardos, B., Cohen, A.L., Fair, D.A., Power, J.D., Church, J.A., Nelson, S.M., Wig, G.S., Vogel, A.C., Lessov-Schlaggar, C.N., Barnes, K.A., Dubis, J.W., Feczko, E., Coalson, R.S., Pruett Jr., J.R., Barch, D.M., Petersen, S.E., Schlaggar, B.L., 2010. Prediction of individual brain maturity using fMRI. Science 329 (5997), 1358–1361, http://dx.doi.org/10.1126/science.1194144.

Dumontheil, I., Apperly, I.A., Blakemore, S.-J., 2010. Online usage of theory of mind continues to develop in late adolescence. Dev. Sci. 13 (2), 331–338, http://dx.doi.org/10.1111/j.1467-7687.2009.00888.x.

Fair, D.A., Cohen, A.L., Dosenbach, N.U.F., Church, J.A., Miezin, F.M., Barch, D.M., Raichle, M.E., Petersen, S.E., Schlaggar, B.L., 2008. The maturing architecture of the brain's default network. Proc. Natl. Acad. Sci. U. S. A. 105 (10), 4028–4032, http://dx.doi.org/10.1073/pnas.0800376105.

Fair, D.A., Cohen, A.L., Power, J.D., Dosenbach, N.U., Church, J.A., Miezin, F.M., Schlaggar, B.L., Petersen, S.E., 2009. Functional brain networks develop from a "local to distributed" organization. PLoS Comput. Biol. 5 (5), e1000381.

Fair, D.A., Dosenbach, N.U.F., Church, J.A., Cohen, A.L., Brahmbhatt, S., Miezin, F.M., Barch, D.M., Raichle, M.E., Petersen, S.E., Schlaggar, B.L., 2007a. Development of distinct control networks through segregation and integration. Proc. Natl. Acad. Sci. U. S. A. 104 (33), 13507–13512, http://dx.doi.org/10.1073/pnas.0705843104.

Fair, D.A., Schlaggar, B.L., Cohen, A.L., Miezin, F.M., Dosenbach, N.U.F., Wenger, K.K., Fox, M.D., Snyder, A.Z., Raichle, M.E., Petersen, S.E., 2007b. A method for using blocked and event-related fMRI data to study "resting state" functional connectivity. Neuroimage 35 (1), 396–405, http://dx.doi.org/10.1016/j.neuroimage.2006.11.051.

Fox, M.D., Raichle, M.E., 2007. Spontaneous fluctuations in brain activity observed with functional magnetic resonance imaging. Nat. Rev. Neurosci. 8 (9), 700–711, http://dx.doi.org/10.1038/nrn2201.

Fox, M.D., Snyder, A.Z., Zacks, J.M., Raichle, M.E., 2005a. Coherent spontaneous activity accounts for trial-to-trial variability in human evoked brain responses. Nat. Neurosci. 9 (1), 23–25.

Fox, M.D., Snyder, A.Z., Vincent, J.L., Corbetta, M., Essen, D.C.V., Raichle, M.E., 2005b. The human brain is intrinsically organized into dynamic, anticorrelated functional networks. Proc. Natl. Acad. Sci. U. S. A. 102 (27), 9673–9678, http://dx.doi.org/10.1073/pnas.0504136102.

Fox, M.D., Zhang, D., Snyder, A.Z., Raichle, M.E., 2009. The global signal and observed anticorrelated resting state brain networks. J. Neurophysiol. 101 (6), 3270–3283, http://dx.doi.org/10.1152/jn.90777.2008.

Gao, W., Alcauter, S., Elton, A., Hernandez-Castillo, C.R., Smith, J.K., Ramirez, J., Lin, W., 2014. Functional network development during the first year: relative sequence and socioeconomic correlations. Cereb. Cortex, http://dx.doi.org/10.1093/cercor/bhu088.

Gordon, E.M., Lee, P.S., Maisog, J.M., Foss-Feig, J., Billington, M.E., VanMeter, J., Vaidya, C.J., 2011. Strength of default mode resting-state connectivity relates to white matter integrity in children. Dev. Sci. 14 (4), 738–751.

Greicius, M.D., Krasnow, B., Reiss, A.L., Menon, V., 2003. Functional connectivity in the resting brain: a network analysis of the default mode hypothesis. Proc. Natl. Acad. Sci. U. S. A. 100 (1), 253–258, http://dx.doi.org/10.1073/pnas.0135058100.

Gusnard, D.A., Akbudak, E., Shulman, G.L., Raichle, M.E., 2001. Medial prefrontal cortex and self-referential mental activity: relation to a default mode of brain function. Proc. Natl. Acad. Sci. U. S. A. 98 (7), 4259–4264, http://dx.doi.org/10.1073/pnas.071043098.

Hallquist, M.N., Hwang, K., Luna, B., 2013. The nuisance of nuisance regression: spectral misspecification in a common approach to resting-state fMRI preprocessing reintroduces noise and obscures functional connectivity. Neuroimage 82, 208–225, http://dx.doi.org/10.1016/j.neuroimage.2013.05.116.

Harris, R.J., Bookheimer, S.Y., Cloughesy, T.F., Kim, H.J., Pope, W.B., Lai, A., Nghiemphu, P.L., Liau, L.M., Ellingson, B.M., 2014. Altered functional connectivity of the default mode network in diffuse gliomas measured with pseudo-resting state fMRI. J. Neurooncol. 116 (2), 373–379.

Heuvel, M.P., van den, Stam, C.J., Kahn, R.S., Pol, H.E.H., 2009. Efficiency of functional brain networks and intellectual performance. J. Neurosci. 29 (23), 7619–7624, http://dx.doi.org/10.1523/JNEUROSCI.1443-09.2009.

Honey, C.J., Thompson, C.R., Lerner, Y., Hasson, U., 2012. Not lost in translation: neural responses shared across languages. J. Neurosci. 32 (44), 15277–15283.

Hwang, K., Hallquist, M.N., Luna, B., 2013. The development of hub architecture in the human functional brain network. Cereb. Cortex 23 (10), 2380–2393, http://dx.doi.org/10.1093/cercor/bhs227.

Jenkinson, M., Bannister, P., Brady, M., Smith, S., 2002. Improved optimization for the robust and accurate linear registration and motion correction of brain images. Neuroimage 17 (2), 825–841, http://dx.doi.org/10.1006/nimg.2002.1132.

Jolles, D.D., Van Buchem, M.A., Crone, E.A., Rombouts, S.A., 2011. A comprehensive study of whole-brain functional connectivity in children and young adults. Cereb. Cortex 21 (2), 385–391.

Jung, R.E., Haier, R.J., 2007. The Parieto-Frontal Integration Theory (P-FIT) of intelligence: converging neuroimaging evidence. Behav. Brain Sci. 30 (2), 135–154, http://dx.doi.org/10.1017/S0140525X07001185, discussion 154-187.

Kelly, A.M.C., Di Martino, A., Uddin, L.Q., Shehzad, Z., Gee, D.G., Reiss, P.T., Margulies, D.S., Castellanos, F.X., Milham, M.P., 2009. Development of anterior cingulate functional connectivity from late childhood to early adulthood. Cereb. Cortex 19 (3), 640–657, http://dx.doi.org/10.1093/cercor/bhn117.

Langeslag, S.J.E., Schmidt, M., Ghassabian, A., Jaddoe, V.W., Hofman, A., van der Lugt, A., Verhulst, F.C., Tiemeier, H., White, T.J.H., 2013. Functional connectivity between parietal and frontal brain regions and intelligence in young children: the Generation R study. Hum. Brain Mapp. 34 (12), 3299–3307, http://dx.doi.org/10.1002/hbm.22143.

Li, C., Tian, L., 2014. Association between resting-state coactivation in the parieto-frontal network and intelligence during late childhood and adolescence. AJNR, http://dx.doi.org/10.3174/ajnr.A3850.

Maddock, R.J., 1999. The retrosplenial cortex and emotion: new insights from functional neuroimaging of the human brain. Trends Neurosci. 22 (7), 310–316, http://dx.doi.org/10.1016/S0166-2236(98)01374-5.

Margulies, D.S., Vincent, J.L., Kelly, C., Lohmann, G., Uddin, L.Q., Biswal, B.B., Villringer, A., Castellanos, F.X., Milham, M.P., Petrides, M., 2009. Precuneus shares intrinsic functional architecture in humans and monkeys. Proc. Natl. Acad. Sci. U. S. A. 106 (47), 20069–20074.

McNealy, K., Mazziotta, J.C., Dapretto, M., 2006. Cracking the language code: neural mechanisms underlying speech parsing. J. Neurosci. 26 (29), 7629–7639, http://dx.doi.org/10.1523/JNEUROSCI.5501-05.2006.

McNealy, K., Mazziotta, J.C., Dapretto, M., 2010. The neural basis of speech parsing in children and adults. Dev. Sci. 13 (2), 385–406.

McNealy, K., Mazziotta, J.C., Dapretto, M., 2011. Age and experience shape developmental changes in the neural basis of language-related learning. Dev. Sci. 14 (6), 1261–1282, http://dx.doi.org/10.1111/j.1467-7687.2011.01075.x.

Menon, V., Uddin, L.Q., 2010. Saliency, switching, and attention and control: a network model of insula function. Brain Struct. Funct. 214 (5–6), 655–667, http://dx.doi.org/10.1007/s00429-010-0262-0.

Miranda-Dominguez, O., Mills, B.D., Grayson, D., Woodall, A., Grant, K.A., Kroenke, C.D., Fair, D.A., 2014. Bridging the gap between the human and macaque connectome: a quantitative comparison of global interspecies structure–function relationships and network topology. J. Neurosci. 34 (16), 5552–5563, http://dx.doi.org/10.1523/JNEUROSCI.4229-13.2014.

Murphy, K., Birn, R.M., Handwerker, D.A., Jones, T.B., Bandettini, P.A., 2009. The impact of global signal regression on resting state correlations: are anti-correlated networks introduced? Neuroimage 44 (3), 893–905, http://dx.doi.org/10.1016/j.neuroimage.2008.09.036.

Nelson, E.E., Leibenluft, E., McClure, E.B., Pine, D.S., 2005. The social re-orientation of adolescence: a neuroscience perspective on the process and its relation to psychopathology. Psychol. Med. 35 (2), 163–174, http://dx.doi.org/10.1017/S0033291704003915.

Petersen, A.C., Crockett, L., Richards, M., Boxer, A., 1988. A self-report measure of pubertal status: reliability, validity, and initial norms. J. Youth Adolesc. 17 (2), 117–133.

Power, J.D., Barnes, K.A., Snyder, A.Z., Schlaggar, B.L., Petersen, S.E., 2012. Spurious but systematic correlations in functional connectivity MRI networks arise from subject motion. Neuroimage 59 (3), 2142–2154, http://dx.doi.org/10.1016/j.neuroimage.2011.10.018.

Raichle, M.E., MacLeod, A.M., Snyder, A.Z., Powers, W.J., Gusnard, D.A., Shulman, G.L., 2001. A default mode of brain function. Proc. Natl. Acad. Sci. U. S.A. 98 (2), 676–682, http://dx.doi.org/10.1073/pnas.98.2.676.

Regev, M., Honey, C.J., Simony, E., Hasson, U., 2013. Selective and invariant neural responses to spoken and written narratives. J. Neurosci. 33 (40), 15978–15988.

Santarnecchi, E., Galli, G., Polizzotto, N.R., Rossi, A., Rossi, S., 2014. Efficiency of weak brain connections support general cognitive functioning. Hum. Brain Mapp., http://dx.doi.org/10.1002/hbm.22495.

Satterthwaite, T.D., Elliott, M.A., Gerraty, R.T., Ruparel, K., Loughead, J., Calkins, M.E., Eickhoff, S.B., Hakonarson, H., Gur, R.C., Gur, R.E., Wolf, D.H., 2013. An improved framework for confound regression and filtering for control of motion artifact in the preprocessing of resting-state functional connectivity data. Neuroimage 64, 240–256, http://dx.doi.org/10.1016/j.neuroimage.2012.08.052.

Satterthwaite, T.D., Wolf, D.H., Loughead, J., Ruparel, K., Elliott, M.A., Hakonarson, H., Gur, R.C., Gur, R.E., 2012. Impact of in-scanner head motion on multiple measures of functional connectivity: relevance for studies of neurodevelopment in youth. Neuroimage 60 (1), 623–632, http://dx.doi.org/10.1016/j.neuroimage.2011.12.063.

Sato, S.M., Schulz, K.M., Sisk, C.L., Wood, R.I., 2008. Adolescents and androgens, receptors and rewards. Horm. Behav. 53 (5), 647–658.

Schlegel, A., 1995. A cross-cultural approach to adolescence. Ethos 23, 15–32.

Schlegel, A., Barry, H., 1991. Adolescence: An Anthropological Inquiry. Free Press, New York.

Seeley, W.W., Menon, V., Schatzberg, A.F., Keller, J., Glover, G.H., Kenna, H., Reiss, A.L., Greicius, M.D., 2007. Dissociable intrinsic connectivity networks for salience processing and executive control. J. Neurosci. 27 (9), 2349–2356, http://dx.doi.org/10.1523/JNEUROSCI.5587-06.2007.

Shulman, G.L., Fiez, J.A., Corbetta, M., Buckner, R.L., Miezin, F.M., Raichle, M.E., Petersen, S.E., 1997. Common blood flow changes across visual tasks: II. Decreases in cerebral cortex. J. Cogn. Neurosci. 9 (5), 648–663, http://dx.doi.org/10.1162/jocn.1997.9.5.648.

Smith, S.M., Fox, P.T., Miller, K.L., Glahn, D.C., Fox, P.M., Mackay, C.E., Filippini, N., Watkins, K.E., Toro, R., Laird, A.R., Beckmann, C.F., 2009. Correspondence of the brain's functional architecture during activation and rest. Proc. Natl. Acad. Sci. U. S. A. 106 (31), 13040–13045, http://dx.doi.org/10.1073/pnas.0905267106.

Smith, S.M., Jenkinson, M., Woolrich, M.W., Beckmann, C.F., Behrens, T.E.J., Johansen-Berg, H., Bannister, P.R., De Luca, M., Drobnjak, I., Flitney, D.E., Niazy, R.K., Saunders, J., Vickers, J., Zhang, Y., De Stefano, N., Brady, J.M., Matthews, P.M., 2004. Advances in functional and structural MR image analysis and implementation as FSL. Neuroimage 23 Suppl. 1, S208–S219, http://dx.doi.org/10.1016/j.neuroimage.2004.07.051.

Smyzer, C.D., Inder, T.E., Shimony, J.S., Hill, J.E., Degnan, A.J., Snyder, A.Z., Neul, J.J., 2010. Longitudinal analysis of neural network development in preterm infants. Cereb. Cortex 20 (12), 2852–2862, http://dx.doi.org/10.1093/cercor/bhq035.

Song, M., Zhou, Y., Li, J., Liu, Y., Tian, L., Yu, C., Jiang, T., 2008. Brain spontaneous functional connectivity and intelligence. Neuroimage 41 (3), 1168–1176, http://dx.doi.org/10.1016/j.neuroimage.2008.02.036.

Sonuga-Barke, E.J.S., Castellanos, F.X., 2007. Spontaneous attentional fluctuations in impaired states and pathological conditions: a neurobiological hypothesis. Neurosci. Biobehav. Rev. 31 (7), 977–986, http://dx.doi.org/10.1016/j.neubiorev.2007.02.005.

Sridharan, D., Levitin, D.J., Menon, V., 2008. A critical role for the right fronto-insular cortex in switching between central-executive and default-mode networks. Proc. Natl. Acad. Sci. U. S. A. 105 (34), 12569–12574, http://dx.doi.org/10.1073/pnas.0800005105.

Stevens, M.C., Pearlson, G.D., Calhoun, V.D., 2009. Changes in the interaction of resting-state neural networks from adolescence to adulthood. Hum. Brain Mapp. 30 (8), 2356–2366, http://dx.doi.org/10.1002/hbm.20673.

Supekar, K., Uddin, L.Q., Prater, K., Amin, H., Greicius, M.D., Menon, V., 2010. Development of functional and structural connectivity within the default mode network in young children. Neuroimage 52 (1), 290–301, http://dx.doi.org/10.1016/j.neuroimage.2010.04.009.

Thomason, M.E., Chang, C.E., Glover, G.H., Gabrieli, J.D.E., Greicius, M.D., Gotlib, I.H., 2008. Default-mode function and task-induced deactivation have overlapping brain substrates in children. Neuroimage 41 (4), 1493–1503, http://dx.doi.org/10.1016/j.neuroimage.2008.03.029.

Uddin, L.Q., Supekar, K., Menon, V., 2010. Typical and atypical development of functional human brain networks: insights from resting-state FMRI. Front. Syst. Neurosci. 4, 21, http://dx.doi.org/10.3389/fnsys.2010.00021.

Uddin, L.Q., Supekar, K.S., Ryali, S., Menon, V., 2011. Dynamic reconfiguration of structural and functional connectivity across core neurocognitive brain networks with development. J. Neurosci. 31 (50), 18578–18589.

Van Dijk, K.R.A., Sabuncu, M.R., Buckner, R.L., 2012. The influence of head motion on intrinsic functional connectivity MRI. Neuroimage 59 (1), 431–438, http://dx.doi.org/10.1016/j.neuroimage.2011.07.044.

Vincent, J.L., Kahn, I., Snyder, A.Z., Raichle, M.E., Buckner, R.L., 2008. Evidence for a frontoparietal control system revealed by intrinsic functional connectivity. J. Neurophysiol. 100 (6), 3328–3342, http://dx.doi.org/10.1152/jn.90355.2008.

von dem Hagen, E.A., Stoyanova, R.S., Baron-Cohen, S., Calder, A.J., 2013. Reduced functional connectivity within and between 'social' resting state networks in autism spectrum conditions. Soc. Cogn. Affect. Neurosci. 8 (6), 694–701.

Wang, L., Song, M., Jiang, T., Zhang, Y., Yu, C., 2011. Regional homogeneity of the resting-state brain activity correlates with individual intelligence. Neurosci. Lett. 488 (3), 275–278, http://dx.doi.org/10.1016/j.neulet.2010.11.046.

Watkins, M.W., Smith, L.G., 2013. Long-term stability of the Wechsler intelligence scale for children—fourth edition. Psychol. Assess. 25 (2), 477–483, http://dx.doi.org/10.1037/a0031653.

Wechsler, D., 1991. The Wechsler Intelligence Scale for Children—Third Edition. The Psychological Corporation, San Antonio, TX.

Wechsler, D., 1999. Wechsler Abbreviated Scale of Intelligence. The Psychological Corporation: Harcourt Brace & Company, New York, NY.

Weil, L.G., Fleming, S.M., Dumontheil, I., Kilford, E.J., Weil, R.S., Rees, G., Dolan, R.J., Blakemore, S.-J., 2013. The development of metacognitive ability in adolescence. Conscious. Cogn. 22 (1), 264–271, http://dx.doi.org/10.1016/j.concog.2013.01.004.

Williams, B.R., Ponesse, J.S., Schachar, R.J., Logan, G.D., Tannock, R., 1999. Development of inhibitory control across the life span. Dev. Psychol. 35 (1), 205–213, http://dx.doi.org/10.1037/0012-1649.35.1.205.